Research Article

Flood Hazard Mapping Using a Multi-Criteria Decision Analysis Approach Over the Indrawati River Basin

Buddha Subedi[1]*, Binu Devkota[1] and Bishal Shrestha[1]

[1] Department of Civil Engineering, Pulchowk Campus, Tribhuvan University, Pulchowk, Lalitpur, Nepal

Abstract: Floods are devastating natural hazards responsible for direct mortality, deterioration of crops, and damage to infrastructure and property. So, their study is crucial for watershed management and mitigation of flood hazards. The main objective of this study was to create a scientifically valid flood hazard map of the Indrawati River Basin (IRB) through the use of the multi-criteria decision analysis approach. Topographical Wetness Index (TWI), Elevation (EL), Slope (SL), Precipitation (PPT), Land Use/Land Cover (LULC), Normalized Difference Vegetation Index (NDVI), Distance from the River (DRI), Distance from the Road (DRO), Drainage Density (DD), and Soil Type (ST) were chosen as flood-triggering factors based on literature review, data availability, and catchment characteristics. The analytic hierarchy process (AHP) method was used for determining the relative weight of each flood causative factor. All these factors were resampled into a 30 m × 30 m pixel size. Based on an evaluation of satellite imagery, 30 flood points were identified in the IRB, and these

points were used as the testing dataset for validating the outcome. Based on results, the IRB has been classified into five different flood susceptible zones; very low, low, moderate, high, and very high. According to the study, 13%, 26%, 30%, 23%, and 8% of the total area are in very low, low, moderate, high, and very high flood susceptible zones, respectively. The Area Under the Curve (AUC) value for the success rate was 0.792. The results of this study will be crucial for concerned parties to design early warning systems and flood risk reduction measures for flood preparedness.

1. Introduction

Floods are highly destructive natural hazards, engendering the loss of lives and properties across the globe (Tsakiris, 2014). Heavy rainfall or snowmelt that causes transient inundation of surrounding areas by overflowing is the major rationale behind its occurrence (Sarkar & Mondal, 2020). It is the leading cause of natural disaster deaths worldwide, with Asia being a major sufferer (Doocy et al., 2013). Statistics also reveal that between 1980-2006, 90% of those affected by the floods with over 45% of water-related disaster fatalities have been from Asia (Adikari et al., 2010). South Asia, with its extensive river systems, is particularly vulnerable to large-scale floods (Adikari et al., 2010). The floods in North India in 2013, the Yangtze River Flood in 2020, and the devastating floods in Thailand in 2011 are just a few examples of the historical flood-related calamities in South Asia (Gale & Saunders, 2013; Sati & Gahalaut, 2013; Wei et al., 2020). Both anthropogenic and natural factors are accountable for cataclysmic flood incidents that result in direct mortality, deterioration of crops, and damage to infrastructure and property as some of their major impacts (Dewan, 2015; Ullah & Zhang, 2020).

The foothills of Nepal are traversed by the river and its tributaries, which mainly originate from the Himalayas, are frequently inundated by severe floods during the monsoon (Dewan, 2015). Seti floods in 2012, glacial lake outburst floods in Bhotekoshi in 2016 and Barun Khola in 2017, Terai floods in 2017, and debris flow in Sindhupalchowk in 2020 are some of the major catastrophic floods to have occurred in Nepal in the past. Heavy flash floods from Melamchi and Indrawati river tributaries in Melamchi Bazar on 15 June 2021 is the major incident in recent times that has taken the life of more than 20 people, washed away more than 100 homes, swept away 12 suspension footbridges and seriously damaged the Melamchi water supply project (The Melamchi Flood Disaster, 2021; Times, 2021) . Fragile geological conditions, climate and topographical extremes, and seismic activities are the natural causes, whereas inappropriate agricultural practices, deforestation, alteration in land use patterns, and many developmental activities are the anthropogenic causes of flooding in Nepalese rivers (Yogacharya & Gautam, 2008).

Modern technology widely involves the use of the Remote Sensing (RS) technique for flood hazard mapping by considering RS data in GIS for preparing spatial databases (Haq et al., 2012). RS data assists us in providing germane information such as vegetation cover, climatic features, topographical features, and many others regarding our region

(Ali et al., 2019). As various factors are responsible for flood occurrence, multi-criteria-based flood susceptibility mapping will be more accurate, reliable, and representative in comparison to single criterion-based flood susceptibility mapping (Minea, 2013). Various methods, such as AHP, Frequency Ratio (FR), Artificial Neural Networks, Support Vector Machines, and Decision Trees, etc., are used for flood hazard mapping in different regions of the world (Das & Gupta, 2021).

AHP is a semi-quantitative method, which is extensively used as a multi-criteria decision analysis (MCDA) approach (Orencio & Fujii, 2013; Wubalem et al., 2021). A pairwise comparison matrix is used for determining the weights of each criterion by solving a broad range of multi-criteria decision-making problems in AHP method (Le Cozannet et al., 2013). The procedures of selecting, comparing, and rating various criteria are the major limitations of the AHP method as it is based on expert opinions and subjectivity (Danumah et al., 2016). The creation of a scientifically valid flood hazard map for the research area is the major goal of this study. Other accompanied objectives include determining the weight of each flood causative element using AHP and validating the flood hazard map using the Receiver Operating Characteristic (ROC) curve. No study has been conducted in the region regarding flood hazard mapping to this date, making this study the first of its kind in the IRB. This study can be expected to be quite helpful for policymakers in mitigating flood hazards.

2. Study Area

IRB, a part of the Indrawati River Basin, was delineated by considering (85°37'43"E, 27°43'34"N) as an outlet point. It is situated in the mid-hills of Nepal and lies within the latitude of $27^043'26''$ N – $28^010'12''$ N and longitude of $85^044'20''$ E – $85^026'58''$ E as shown in Figure 1. The elevation of our basin ranges from 688 m – 6188 m. The Indrawati River is the major river of our basin which originates in the High Himalayas at an elevation of about 5850 m above mean sea level (AMSL) and confluences with the Sun Koshi River at an elevation of 626 m above mean sea level into the Koshi River basin, which eventually connects with the Ganges River in Northern India (Karki,2005). The Larke Khola, Yangri Khola, Melamchi Khola, Jhyangri Khola, Chaa Khola, Handi Khola, and Mahadev Khola are the 7 major tributaries that contribute to the flow of the Indrawati River (Bhattarai et al., 2002). IRB has a catchment area of 966 sq. km.
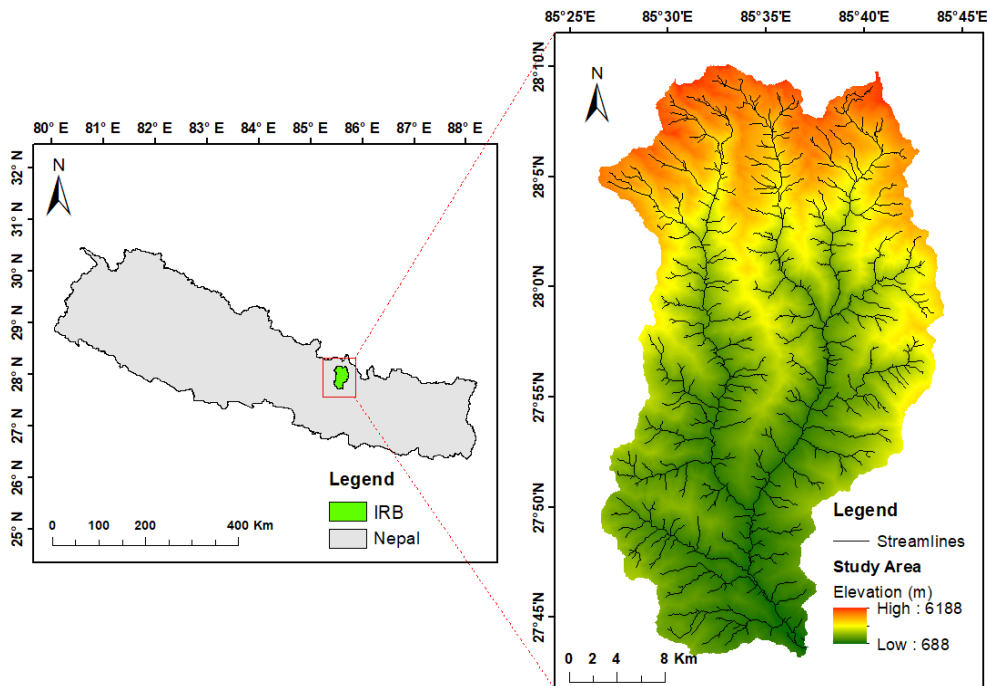
Figure 1. *Location of study area*

The basin is situated in the Himalayan region's subtropical to alpine climate zone (Bhattarai et al., 2002). The interplay between the South Asian monsoon system and the Himalayas significantly determines the climate in the basin (Bartlett et al., 2011). The summer months, roughly from mid-May to mid-October, are marked by heavy rain, relatively high temperatures, and humidity. The average annual rainfall of the basin ranges from 3,874 mm to 1,128 mm, about half of which falls in the months of July and August. Only around 7% of the total annual rainfall falls from November to April, making the rest of the year significantly drier and the temperature of the basin ranges from 5°C – 32.5°C, while the relative humidity ranges from 60% in the dry season to 90% in the wet season, with the average value being about 70% (Bhattarai et al., 2002; Sharma, 2002). The two discharge gauging stations within the basin, Helambu and Dolalghat, estimated the Melamchi river's annual average flow of 10.21 m³/s and the Indrawati river's flow of 75.06 m³/s. (Shrestha et al., 2016). The catchment area of the basin has a wide range of land use, with around 53.13%, 1.77%, 16.02%, 20.27%, 4.94%, 0.14% and 3.73% of forest, shrub land, grassland, agricultural area, barren land, water body and snow/glacier respectively as per data of 2010 given by The International Centre for Integrated Mountain Development (ICIMOD). The region was ravaged by the flood of 2021, which makes it very necessary to produce the flood hazard map of the area so that the unprecedented damage that occurred in 2021 would not be replicated again in the future (The Melamchi Flood Disaster, 2021).

3. Methodology

In the present study, the MCDA has been adopted, consisting of ten indicators, to compute the flood hazard index (FHI) of our study area in the GIS environment. The spatially distributed maps were created using information from secondary sources, and the final hazard map was prepared and validated using the receiver operating characteristics (ROC) method. The basic methodological framework is shown in Figure 2.
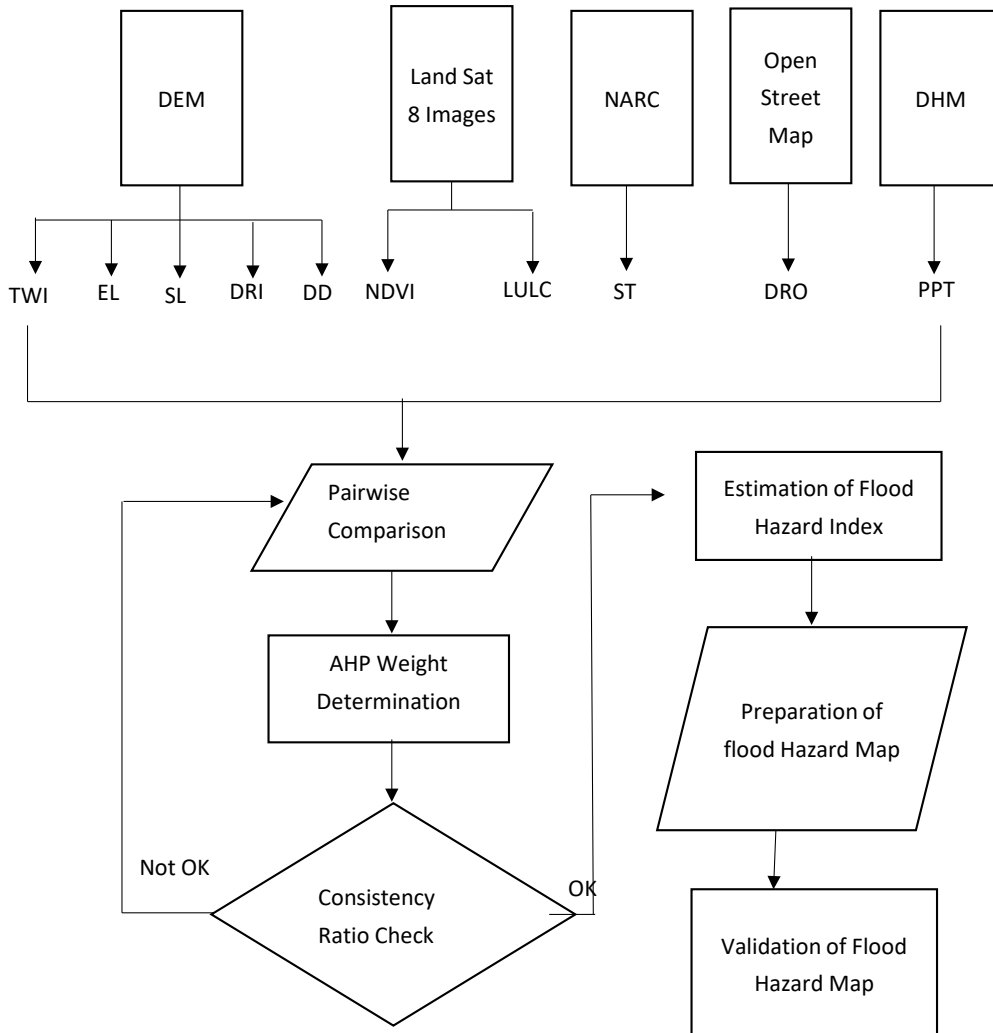
Figure 2: *Methodological framework for flood hazard mapping (Note: TWI = Topographical Wetness Index, EL = Elevation, SL = Slope, DRI = Distance from the River, DD = Drainage Density, NDVI = Normalized Difference Vegetation Index, LULC = Land Use/Land Cover, ST = Soil Type, DRO = Distance from the Road, PPT = Precipitation)*

3.1 Flood Causative Factors and Data Sources

Proper selection of flood causative factors is very crucial to prepare an accurate and representative flood hazard map (Kia et al., 2012). It is a challenging task to choose various flood driving parameters for flood hazard mapping (Ali et al., 2019). Flood triggering factors were determined based on literature review, data availability, and physical and natural characteristics of the study area (Khosravi et al., 2016). TWI, EL, SL, PPT, LULC, NDVI, DRI, DRO, DD, and ST are considered flood causative factors of our study area. The relationship of each causative factors with flood susceptibility along with the formulas and data required for the preparation of flood hazard map have been presented in Table 1.

Table 1. *Flood causative factors, their preparation and relationship with flood susceptibility*

Flood Triggering Factors	Preparation of Flood Causative Factors and its Relationship with Flood Susceptibility
TWI	It describes the spatial distribution of wetness and regulates the flow of water overland (Samanta et al., 2018). TWI maps define the effect of topography on the quantity of wet levels that form runoff and are used to investigate the flood potential of watersheds (Haghizadeh et al., 2017). TWI map was prepared from a digital elevation model (DEM) of 30m × 30m resolution in a GIS environment using the following formula (Ullah & Zhang, 2020); $$TWI = \left[\frac{As}{\tan(\beta)} \right] \qquad (1)$$ Where, β is the slope gradient and As is the upstream contributing area. • Low values of TWI correspond to an area of less runoff and water accumulation (Fernández & Lutz, 2010)
Elevation	• Land elevation has a remarkable role in flood hazard mapping as it governs temperature as well as rainfall of any area (Fernández & Lutz, 2010; Samanta et al., 2012). • The elevation map was prepared from DEM of 30m × 30m resolution in a GIS environment. • The higher the value of elevation, the lesser will be its susceptibility to flood (Das, 2018).
Slope	• It has conspicuous effects on flood hazard mapping as it regulates the flow of surface water which ultimately controls percolation in the vertical direction and soil erosion (Jahangir et al., 2019). • Slope map was prepared in a GIS environment from DEM of 30m × 30m resolution. • Steep areas associated with lower slopes are usually less prone to flood and vice versa (Seejata et al., 2018).

Precipitation	• Daily rainfall data was obtained from DHM, from which a rainfall distribution map was prepared from average annual rainfall using Inverse Distance Weighting (IDW) interpolation in GIS Environment. • Higher rainfall prompts greater discharge in a river and may cause flash floods if a huge amount of rainfall happens in a short time period (Paul et al., 2019; Ullah & Zhang, 2020).
LULC	• Supervised classification technique was used for preparing the LULC map from Landsat-8 OLI satellite imagery (Samanta et al., 2018). • Runoff speed and extent as well as terrain infiltration, which has a significant contribution to the occurrence of floods is dependent upon LULC (Khosravi et al., 2016). • The LULC map was categorized into six classes: water, barren, forest, planted/cultivated, snow and others. Other class mainly include the area eclipsed by the cloud.
NDVI	• NDVI map was obtained from Landsat_8 data of study area using the equation 2 provided below; NDVI = (NIR - VIS)/(NIR + VIS) (2) Where, NIR and VIS are the spectral reflectance measurement acquired in the near-infrared and visible (red) region respectively (Khosravi et al., 2016). • Values of NDVI normally range from -1 to 1 (Ullah & Zhang, 2020). • Vegetation reduces the runoff and acts as an opposing factor against floods (Tehrany et al., 2014). • NDVI of our region ranges from -0.215 to 0.519. • The higher positive value of NDVI indicates less susceptibility to flooding.
Distance From the River	• Distance from the river has a patently visible role in flood hazard mapping (Glenn et al., 2012). • DEM of 30m × 30m resolution in GIS environment was used to derive the streamlines after which Euclidean distance tool available in ArcGIS software was used to derive distance from river map. • The greater the distance from the river, the lesser will be its proneness to floods.
Distance From the Road	• Open Street Map was used for obtaining information related to road networks (Uddin & Matin, 2021). • Distance from the road was calculated using the Euclidean distance tool available in ArcGIS software. • The higher the distance from the road, the lesser will be the susceptibility to floods.
Drainage Density	• It is defined as the total length of the channel per unit area (Dragičević et al., 2019; HORTON, 1945). • Drainage density map was prepared from DEM of 30m × 30m resolution in a GIS environment and was classified into five classes using natural break. • More drainage density indicates greater surface runoff and hence higher possibility of floods (Ali et al., 2019).

Soil Type	• Soil type refers to the various categories of soil in the study area which has a patently visible role in the flood hazard mapping. • Soil Map was obtained from NARC. • Soils of the study area are categorized into Leptosols (Gaelic), Regosols (Eutric) and Cambisols (Eutric, Humic, Chromic and Gleyic). • Soil type and its texture affects the moisture-holding capacity and the surface runoff/infiltration.

3.2 Estimation of Weights

The AHP method, a general theory of measurement, has been widely used in resource allocation, planning, and multi-criteria decision making (MCDM) (Saaty, 1990). The fundamental idea behind the analytical hierarchy process is to create a matrix that expresses the relative significance of the selected factors, which provides a basis for the decision-maker (Saaty, 1987).

In this study, the AHP method was adopted for assigning the weights to each of the factors. The selected factors have been weighed on a numerical scale of 1 to 9, as shown in Table 2, which was adopted from Saaty(1990). To get an insight into the relative importance of different flood deriving factors, the weight factors were determined from the pairwise comparison of each element based on the available literature and field data obtained from secondary sources (Bartlett et al., 2011; Karki, 2005). The pairwise comparison matrix as depicted in Table 3, was constructed based on the weights, where one alternative's rank value in the matrix is reciprocal to its inverse comparison.

Table 2. Numerical Scale for the selection of the flood comparison factor (Saaty, 1990)

Definition	Intensity of importance
Extremely important	9
Very strongly important	7
Strongly more important	5
Moderately more important	3
Equally important	1

Table 3. Pairwise comparison matrix: Analytical Hierarchy Process

Parameters	TWI	EL	SL	PPT	LULC	NDVI	DRI	DRO	DD	ST
TWI	1	1	1	1	3	5	1	3	1	1
EL	1	1	1	1	2	3	1	3	1	1
SL	1	1	1	1	3	1	1/2	1	1	1
PPT	1	1	1	1	3	2	2	3	1	1
LULC	1/3	1/2	1/3	1/3	1	1	1/3	3	1	1
NDVI	1/5	1/3	1	1/2	1	1	1/5	1	1	1
DRI	1	1	2	1/2	3	5	1	3	1	1
DRO	1/3	1/3	1	1/3	1/3	1	1/3	1	1	1
DD	1	1	1	1	1	1	1	1	1	1
ST	1	1	1	1	1	1	1	1	1	1

Table 4. *Normalized comparison matrix: Analytical Hierarchy Process*

Parameters	TWI	EL	SL	PPT	LULC	NDVI	DRI	DRO	DD	ST	Normalized Principle Eigen Vector (%)
TWI	0.13	0.12	0.1	0.13	0.16	0.24	0.12	0.15	0.1	0.1	13.48
EL	0.13	0.12	0.1	0.13	0.11	0.14	0.12	0.15	0.1	0.1	11.98
SL	0.13	0.12	0.1	0.13	0.16	0.05	0.06	0.05	0.1	0.1	9.98
PPT	0.13	0.12	0.1	0.13	0.16	0.1	0.24	0.15	0.1	0.1	13.25
LULC	0.04	0.06	0.03	0.13	0.05	0.05	0.04	0.15	0.1	0.1	6.71
NDVI	0.03	0.04	0.1	0.04	0.05	0.05	0.02	0.05	0.1	0.1	6.04
DRI	0.13	0.12	0.19	0.07	0.16	0.24	0.12	0.15	0.1	0.1	13.8
DRO	0.04	0.04	0.1	0.07	0.02	0.05	0.04	0.05	0.1	0.1	5.79
DD	0.13	0.12	0.1	0.04	0.05	0.05	0.12	0.05	0.1	0.1	9.48
ST	0.13	0.12	0.1	0.13	0.05	0.05	0.12	0.05	0.1	0.1	9.48

In the AHP, the judgment is based on evaluating two items on a single attribute without taking into account other properties or other elements. To assess the consistency of using the scale, the factor weight values for the categorized sub-factors must be determined. If w is the weight vector (Eigen vector) and λ is the eigenvalue of the comparison matrix A, then the Eigen vector can be represented by the equation 3. The necessary and sufficient condition for matrix A to be consistent is that the principal Eigen value, λ_{max} is equal to the number of the factors (Saaty, 1990).

$$Aw = \lambda w \qquad (3)$$

The consistency index (CI), which is the variance of the error incurred in estimating 'n' numbers of parameters of the matrix is given by equation 4 and consistency ratio (CR) was calculated using equation 5.

$$C.I. = \frac{\lambda_{max} - n}{n-1} \qquad (4)$$

$$CR = \left(\frac{CI}{RI}\right) \qquad (5)$$

Where CR is the consistency ratio, CI is the consistency index, and RI is the random index, based on the number of parameters given by Saaty(1990). Saaty also suggested that the estimate of the weights can only be accepted if the CI is less than 0.1; otherwise, we must attempt to improve the consistency (Saaty, 1990;Saaty & Vargas, 2012).

The principal Eigen value computed by the summation of products between the normalized relative weight - sum of the column of the initial matrix as shown in Table 3 and the normalized Eigen vector (Table 4) was 10.79. For n =10, CI was calculated to be 0.09 and CR to be 0.06 given that RI =1.49. Since the computed value of CR ≤ 0.1, which ratifies the assumptions made to build a pairwise matrix.

3.3 Preparation of Flood Hazard Map

Flood hazard map was prepared based on flood hazard index (FHI), which is calculated from equation 6 provided below (Seejata et al., 2018).

$$FHI = \sum_{i=1}^{n} r_i w_i \qquad (6)$$

Where, η, w_i, and n are the rating of parameter in each unit, the weight of parameter and the number of criteria respectively, rating of each unit of every parameter is depicted in Table 5 provided below. Each flood criterion was divided into five susceptibility class ranges using the natural break method in ArcGIS (Ullah & Zhang, 2020). Ratings in Table 5 refer to the possible low and high contribution to the flood hazard.

Table 5. Range of values for five different flood susceptibility class of each criterion with their rating

Flood Causative Criterion	Unit	Range	Susceptibility Class	Rating
TWI	Unitless	-9.621 - -6.66	Very Low	1
		-6.66 - -5.093	Low	2
		-5.093 - -2.916	Moderate	3
		-2.916 - 0.916	High	4
		0.916 - 12.671	Very High	5
EL	M	688 - 1586	Very High	5
		1586-2396	High	4
		2396-3332	Moderate	3
		3332-4336	Low	2
		4336-6188	Very Low	1
SL	%	0 - 15.297	Very High	5
		15.297 - 24.124	High	4
		24.124 - 32.408	Moderate	3
		32.408 - 42.525	Low	2
		42.525 - 78.723	Very Low	1
PPT	mm	1759.851 - 2066.541	Very Low	1
		2066.541 - 2290.583	Low	2
		2290.583 - 2466.713	Moderate	3
		2466.713 - 2607.473	High	4
		2607.473 - 2845.114	Very High	5

LULC		Water	Very High	5
		Snow	High	4
		Barren	Moderate	3
		Agriculture and Forest	Low	2
		Others	Very Low	1
NDVI	Unitless	-0.215 - 0.026	Very High	5
		0.026 - 0.121	High	4
		0.121 - 0.198	Moderate	3
		0.198- 0.287	Low	2
		0.287 - 0.519	Very Low	1
DRI	m	0 - 182.483	Very High	5
		182.483 - 375.899	High	4
		375.899 - 582.495	Moderate	3
		582.495 - 825.409	Low	2
		825.409 - 1570.637	Very Low	1
DRO	m	0 - 829.759	Very High	5
		829.759 - 2412.343	High	4
		2412.343 - 4508.492	Moderate	3
		4508.492 - 6921.878	Low	2
		6921.878 - 10959.242	Very Low	1
DD	m/Km^2	0 - 559.693	Very Low	1
		559.693 - 1270.073	Low	2
		1270.073 - 2066.559	Moderate	3
		2066.559 - 3142.892	High	4
		3142.892 - 5510.825	Very High	5
ST		Lpi	Very Low	1
		Cmu	Low	2
		Rge	Moderate	3
		Cme and Cmx	High	4
		Cmg	Very High	5

3.4 Validation of Flood Hazard Map

The receiver operating characteristic (ROC) curve was used for the validation of the prediction map as it produced clear and representative results (Ullah & Zhang, 2020). First, the inundated area was determined from satellite images using PlanetScope and then 30 historical flood points were identified in the IRB after digitalization of the inundated area into a polygon in ArcGIS. Historical flood data was juxtaposed with the obtained flood hazard map to validate our results (Janizadeh et al., 2019).

4. Results and Discussions

4.1 Relative Weight of Flood Criterions

In the determination of flood susceptibility of the region, the distance from the river, which had the greatest weightage, 13.8% as per the AHP method, had the highest contribution to the flooding, closely followed by TWI and precipitation, with weightages of 13.28% and 13.25% respectively. Elevation, slope drainage density, and soil type had moderate effects on the occurrence of the flood with the weight of 11.98%, 9.98%, 9.48%, and 9.48% respectively, whereas LULC, NDVI, and distance from the road are the factors with a low level of influence on flood susceptibility with the weight of 6.71%, 6.04%, and 5.79% as per the calculation depicted in Table 4, and this can be judged as reasonable by examining the final flood hazard map and flood susceptibility map of each criterion as provided in Figure 3 and Figure 4. Frequent floods during periods of heavy precipitation in Melamchi Bazar, which is nearer to the Melamchi River, corroborate our findings that the DRI and PPT contribute more to flood susceptibility. As proper assessment of flood hazard areas is required for flood management strategy, the relative importance of each criterion plays an important role in identifying such flood prone areas.

4.2 Flood Hazard Map

The flood hazard index (FHI) used for creating flood hazard map of the study area was found to lie in the range 160-485. Using the natural break method, for each criterion, in ArcGIS the total area was divided into five categories of risk, namely very low, low, moderate, high, and very high as depicted in Figure 3. As per the study, 13%, 26%, 30%, 23%, and 8% of the total area lie respectively, in very low, low, moderate, high and very high flood susceptible zones as exhibited by Figure 4. Flood susceptibility map of distance from the river criterion resembles largely to final flood hazard map. Particularly, the area in the vicinity of the Melamchi- Khola in the central-western part of the basin, which includes places like Pokhari Danda, Chanaute, and Naubise Taar and the area in the southern part of the basin in the vicinity of the Indrawati river including places like Thadkhol and Bhimtar are found to have a high level of the flood hazard. Low, elevation, less slope, barren land and less distance from river has jointly contributed for high flood susceptibility in these regions. In addition, the central part of the basin, which mainly includes Melamchi Bazar, a largely populated region of the basin is more prone to the very high level of flood hazard. School, municipality office and Melamchi playground are even in risk along with agricultural and settlement area as this small region is surrounded by Mealmchi-Khola from one side and the Indrawati River from two sides. Although the northern region of the basin receives a fairly greater proportion of the precipitation, the flood susceptibility of those areas were less due to the greater elevation and the steep slope of the area.

4.3 Validation of Flood Hazard Map

Validation of the flood hazard map is a crucial process to ensure the accuracy of obtained results. The ROC curve obtained using historical flood is shown in Figure 5, and the AUC value for the success rate was found to be 0.792. Although the AUC

value is reasonable, it might be possible that we might have excluded some flood triggering factors having considerable effects on flood susceptibility. The coarseness of DEM as well as the process of determining the related weight of each criterion might have resulted in some unrepresentative results. Further research is necessary to map flood hazard by different methods considering different flood causative factors and by using DEM data of different resolutions, which will help to more accurately assess flood hazard maps.
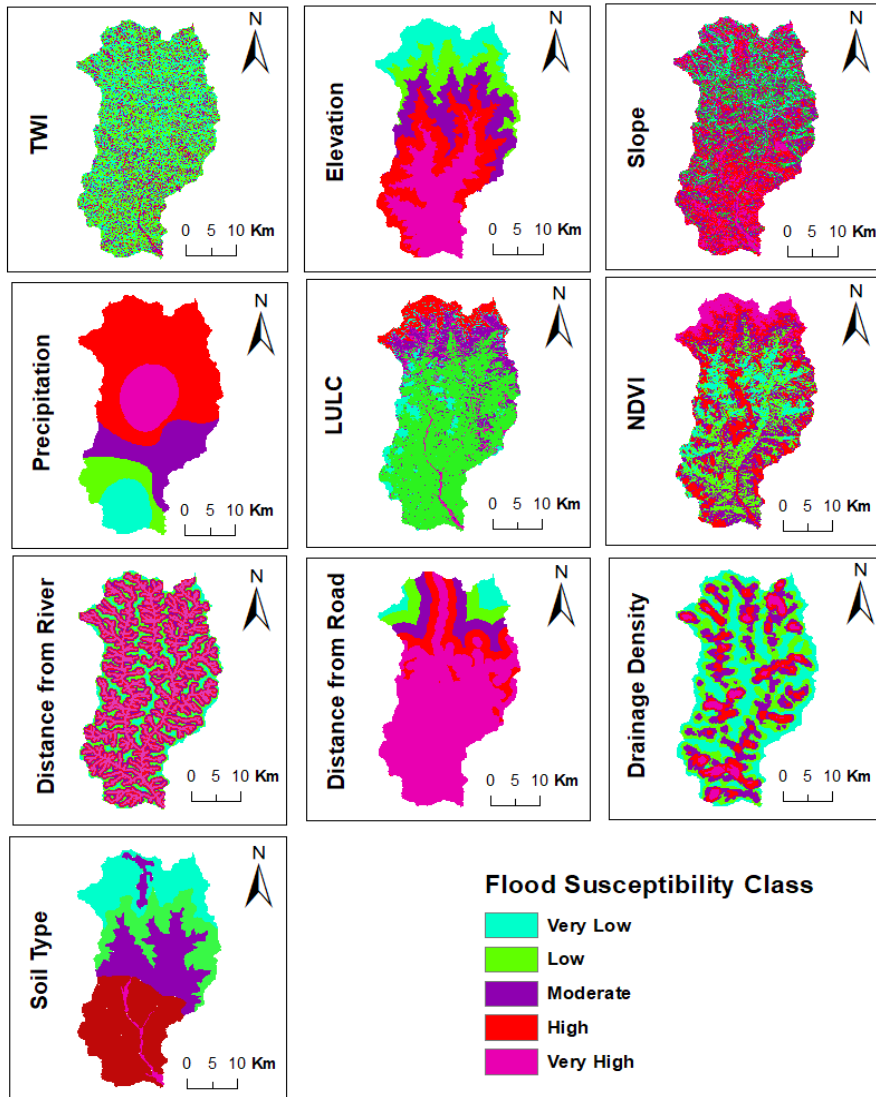
Figure 3. *Classification of the selected factors in the Indrawati River Basin*
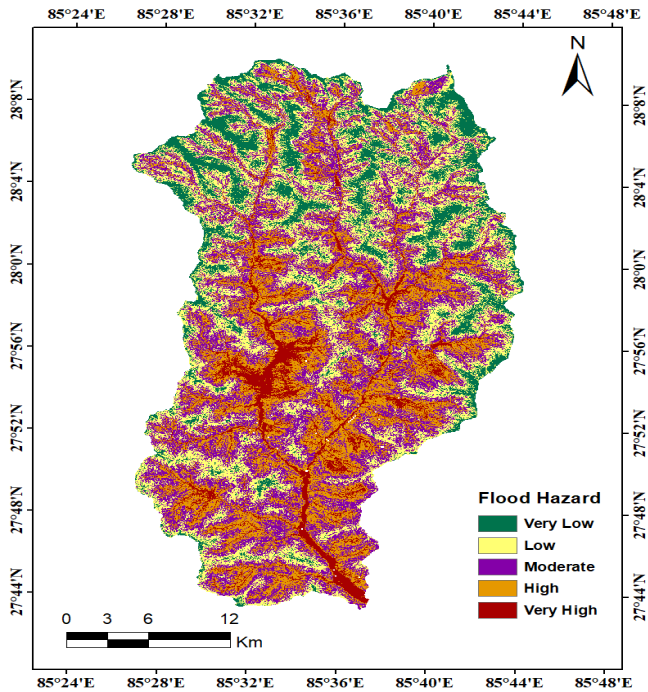
Figure 4. Flood Hazard Map of Indrawati River Basin from AHP
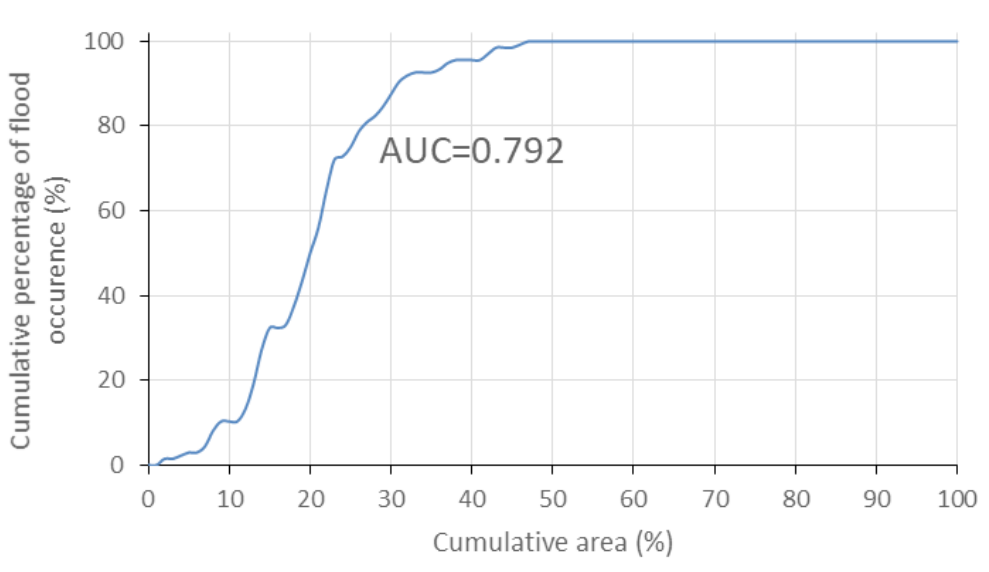

Figure 5. ROC curve for the validation of flood hazard map

5. Conclusions

Flood Hazard Mapping is a crucial tool for the water resources and land use planning and management, which helps to assess the need for new and improved infrastructure to reduce the vulnerability of the population to flooding events in the future. AHP and a geospatial approach were used to demarcate the flood prone areas in the IRB. TWI, EL, SL, PPT, LULC, NDVI, DRI, DRO, DD, and ST were considered as the major flood causative factors for which the consistency ratio was calculated to be 9%. It verifies the consistency used in the estimation of the parameters. Also, the AUC for the ROC method indicates the reasonable accuracy of the prediction systems used for the preparation of the flood hazard map. Thus, the flood susceptibility map prepared in this study can be used by the planners and engineers to develop risk management and mitigation plans for the study area.

The flood hazard map clearly depicts that the areas in the vicinity of the river with lower elevation, low slope, and low TWI are most vulnerable to flooding. The central- western, and southern parts of the basin are particularly more vulnerable to the floods. These are the areas with great numbers of human settlements, thereby making them particularly more vulnerable to human casualties during the floods. Thus, stern measures like the construction of dams, embankments, and other river training measures must be adopted to prevent flooding in the areas. The uncontrolled urbanization in the vicinity of the rivers must be controlled. Proper evacuation and planning measures must be ensured in the areas with a moderate or high level of flood hazard, whereas settlement around the areas with a very high level of flood hazard must be shifted to the safer zones.

Our study considers ten flood-causative factors; however, further research incorporating several other factors related to vegetation and land use like crop type and agricultural practices along with their weights will be helpful in producing highly accurate and representative results. More reliable information about the precipitation and peak flow discharges of the area, along with the consideration of their changes in the future scenario due to climate change, will help in the development of the models with a higher degree of accuracy in mapping flood hazards.

Author's Contributions:
The first two authors have equal contributions.
Conflicts of Interest: The authors declare no conflict of interest.

References

Adikari, Y., Osti, R., & Noro, T. (2010). Flood-related disaster vulnerability: An impending crisis of megacities in Asia: Flood Vulnerability in Asian Megacities. *Journal of Flood Risk Management*, *3*(3), 185–191. https://doi.org/10.1111/j.1753-318X.2010.01068.x

Ali, S. A., Khatun, R., Ahmad, A., & Ahmad, S. N. (2019). Application of GIS-based analytic hierarchy process and frequency ratio model to flood vulnerable mapping and risk area

estimation at Sundarban region, India. *Modeling Earth Systems and Environment*, *5*(3), 1083–1102. https://doi.org/10.1007/s40808-019-00593-z

Bartlett, R., Freeman, S., Cook, J., Dongol, B. S., Sherchan, R., Shrestha, M., & McCornick, P. G. (2011). *Freshwater ecosystem vulnerability assessment: The Indrawati sub-basin, Nepal* (p. 48). Nicholas Institute for Environmental Policy Solutions Report, NI R 11-07, Duke University, WWF.

Bhattarai, M., Pant, D., Mishra, V. S., Devkota, H., Pun, S., Kayastha, R. N., & Molden, D. (2002). Integrated development and management of water resources for productive and equitable use in the Indrawati River Basin, Nepal. *International Water Management Institute (IWMI)*. http://dx.doi.org/10.3910/2009.177

Danumah, J. H., Odai, S. N., Saley, B. M., Szarzynski, J., Thiel, M., Kwaku, A., Kouame, F. K., & Akpa, L. Y. (2016). Flood risk assessment and mapping in Abidjan district using multi-criteria analysis (AHP) model and geoinformation techniques, (cote d'ivoire). *Geoenvironmental Disasters*, *3*(1), 10. https://doi.org/10.1186/s40677-016-0044-y

Das, S., & Gupta, A. (2021). Multi-criteria decision based geospatial mapping of flood susceptibility and temporal hydro-geomorphic changes in the Subarnarekha basin, India. *Geoscience Frontiers*, *12*(5), 101206. https://doi.org/10.1016/j.gsf.2021.101206

Dewan, T. H. (2015). Societal impacts and vulnerability to floods in Bangladesh and Nepal. *Weather and Climate Extremes*, *7*, 36–42. https://doi.org/10.1016/j.wace.2014.11.001

Doocy, S., Daniels, A., Murray, S., & Kirsch, T. D. (2013). The Human Impact of Floods: A Historical Review of Events 1980-2009 and Systematic Literature Review. *PLoS Currents*. https://doi.org/10.1371/currents.dis.f4deb457904936b07c09daa98ee8171a

Dragičević, N., Karleuša, B., & Ožanić, N. (2019). Different Approaches to Estimation of Drainage Density and Their Effect on the Erosion Potential Method. *Water*, *11*(3), 593. https://doi.org/10.3390/w11030593

Fernández, D. S., & Lutz, M. A. (2010). Urban flood hazard zoning in Tucumán Province, Argentina, using GIS and multicriteria decision analysis. *Engineering Geology*, *111*(1–4), 90–98. https://doi.org/10.1016/j.enggeo.2009.12.006

Gale, E. L., & Saunders, M. A. (2013). The 2011 Thailand flood: Climate causes and return periods. *Weather*, *68*(9), 233–237. https://doi.org/10.1002/wea.2133

Glenn, E. P., Morino, K., Nagler, P. L., Murray, R. S., Pearlstein, S., & Hultine, K. R. (2012). Roles of saltcedar (Tamarix spp.) and capillary rise in salinizing a non-flooding terrace on a flow-regulated desert river. *Journal of Arid Environments*, *79*, 56–65. https://doi.org/10.1016/j.jaridenv.2011.11.025

Haghizadeh, A., Siahkamari, S., Haghiabi, A. H., & Rahmati, O. (2017). Forecasting flood-prone areas using Shannon's entropy model. *Journal of Earth System Science*, *126*(3), 39. https://doi.org/10.1007/s12040-017-0819-x

Haq, M., Akhtar, M., Muhammad, S., Paras, S., & Rahmatullah, J. (2012). Techniques of Remote Sensing and GIS for flood monitoring and damage assessment: A case study of Sindh province, Pakistan. *The Egyptian Journal of Remote Sensing and Space Science*, *15*(2), 135–141. https://doi.org/10.1016/j.ejrs.2012.07.002

Horton, R. E. (1945). EROSIONAL DEVELOPMENT OF STREAMS AND THEIR DRAINAGE BASINS; HYDROPHYSICAL APPROACH TO QUANTITATIVE MORPHOLOGY. *Geological Society of America Bulletin*, *56*(3), 275. https://doi.org/10.1130/0016-7606(1945)56[275:EDOSAT]2.0.CO;2

Jahangir, M. H., Mousavi Reineh, S. M., & Abolghasemi, M. (2019). Spatial predication of flood zonation mapping in Kan River Basin, Iran, using artificial neural network algorithm. *Weather and Climate Extremes*, *25*, 100215. https://doi.org/10.1016/j.wace.2019.100215

Janizadeh, S., Avand, M., Jaafari, A., Phong, T. V., Bayat, M., Ahmadisharaf, E., Prakash, I., Pham, B. T., & Lee, S. (2019). Prediction Success of Machine Learning Methods for Flash Flood Susceptibility Mapping in the Tafresh Watershed, Iran. *Sustainability*, *11*(19), 5426. https://doi.org/10.3390/su11195426

Karki, A. (2005). Indrawati River Basin Study. *Consolidated Management Services Nepal (CMS)*, 25.

Khosravi, K., Nohani, E., Maroufinia, E., & Pourghasemi, H. R. (2016). A GIS-based flood susceptibility assessment and its mapping in Iran: A comparison between frequency ratio and weights-of-evidence bivariate statistical models with multi-criteria decision-making technique. *Natural Hazards*, *83*(2), 947–987. https://doi.org/10.1007/s11069-016-2357-2

Kia, M. B., Pirasteh, S., Pradhan, B., Mahmud, A. R., Sulaiman, W. N. A., & Moradi, A. (2012). An artificial neural network model for flood simulation using GIS: Johor River Basin, Malaysia. *Environmental Earth Sciences*, *67*(1), 251–264. https://doi.org/10.1007/s12665-011-1504-z

Le Cozannet, G., Garcin, M., Bulteau, T., Mirgon, C., Yates, M. L., Méndez, M., Baills, A., Idier, D., & Oliveros, C. (2013). An AHP-derived method for mapping the physical vulnerability of coastal areas at regional scales. *Natural Hazards and Earth System Sciences*, *13*(5), 1209–1227. https://doi.org/10.5194/nhess-13-1209-2013

Minea, G. (2013). Assessment of the flash flood potential of Bâsca River Catchment (Romania) based on physiographic factors. *Open Geosciences*, *5*(3). https://doi.org/10.2478/s13533-012-0137-4

Orencio, P. M., & Fujii, M. (2013). A localized disaster-resilience index to assess coastal communities based on an analytic hierarchy process (AHP). *International Journal of Disaster Risk Reduction*, *3*, 62–75. https://doi.org/10.1016/j.ijdrr.2012.11.006

Paul, G. C., Saha, S., & Hembram, T. K. (2019). Application of the GIS-Based Probabilistic Models for Mapping the Flood Susceptibility in Bansloi Sub-basin of Ganga-Bhagirathi River and Their Comparison. *Remote Sensing in Earth Systems Sciences*, *2*(2–3), 120–146. https://doi.org/10.1007/s41976-019-00018-6

Rahmati, O., Haghizadeh, A., Pourghasemi, H. R., & Noormohamadi, F. (2016). Gully erosion susceptibility mapping: The role of GIS-based bivariate statistical models and their comparison. *Natural Hazards*, *82*(2), 1231–1258. https://doi.org/10.1007/s11069-016-2239-7

Rahmati, O., Haghizadeh, A., & Stefanidis, S. (2016). Assessing the Accuracy of GIS-Based Analytical Hierarchy Process for Watershed Prioritization; Gorganrood River Basin, Iran. *Water Resources Management*, *30*(3), 1131–1150. https://doi.org/10.1007/s11269-015-1215-4

Saaty, R. W. (1987). The analytic hierarchy process—What it is and how it is used. *Mathematical Modelling*, *9*(3–5), 161–176. https://doi.org/10.1016/0270-0255(87)90473-8

Saaty, T. L. (1990). How to make a decision: The analytic hierarchy process. *European Journal of Operational Research*, *48*(1), 9–26. https://doi.org/10.1016/0377-2217(90)90057-I

Saaty, T. L., & Vargas, L. G. (2012). *Models, methods, concepts & applications of the analytic hierarchy process* (2. ed). Springer.

Samanta, R. K., Bhunia, G. S., Shit, P. K., & Pourghasemi, H. R. (2018). Flood susceptibility mapping using geospatial frequency ratio technique: A case study of Subarnarekha River Basin, India. *Modeling Earth Systems and Environment*, *4*(1), 395–408. https://doi.org/10.1007/s40808-018-0427-z

Samanta, S., Pal, D. K., Lohar, D., & Pal, B. (2012). Interpolation of climate variables and temperature modeling. *Theoretical and Applied Climatology*, *107*(1–2), 35–45. https://doi.org/10.1007/s00704-011-0455-3

Sarkar, D., & Mondal, P. (2020). Flood vulnerability mapping using frequency ratio (FR) model: A case study on Kulik river basin, Indo-Bangladesh Barind region. *Applied Water Science*, *10*(1), 17. https://doi.org/10.1007/s13201-019-1102-x

Sati, S. P., & Gahalaut, V. K. (2013). The fury of the floods in the north-west Himalayan region: The Kedarnath tragedy. *Geomatics, Natural Hazards and Risk*, *4*(3), 193–201. https://doi.org/10.1080/19475705.2013.827135

Seejata, K., Yodying, A., Wongthadam, T., Mahavik, N., & Tantanee, S. (2018). Assessment of flood hazard areas using Analytical Hierarchy Process over the Lower Yom Basin, Sukhothai Province. *Procedia Engineering*, *212*, 340–347. https://doi.org/10.1016/j.proeng.2018.01.044

Sharma, C. (2002). *Effect of Melamchi Water Supply Project on Soil and Water Conservation in the Indrawati River Basin, Nepal*. 6.

Shrestha, S., Shrestha, M., & Babel, Mukand. S. (2016). Modelling the potential impacts of climate change on hydrology and water resources in the Indrawati River Basin, Nepal. *Environmental Earth Sciences*, *75*(4), 280. https://doi.org/10.1007/s12665-015-5150-8

Tehrany, M. S., Lee, M.-J., Pradhan, B., Jebur, M. N., & Lee, S. (2014). Flood susceptibility mapping using integrated bivariate and multivariate statistical models. *Environmental Earth Sciences*, *72*(10), 4001–4015. https://doi.org/10.1007/s12665-014-3289-3

The Melamchi flood disaster: Cascading hazard and the need for Multihazard Risk Management. ICIMOD. (2021, August 17). https://www.icimod.org/article/the-melamchi-flood-disaster/

Times, N. (2021). *The monsoon mess in Melamchi*. https://www.nepalitimes.com/latest/the-monsoon-mess-in-melamchi/

Tsakiris, G. (2014). Flood risk assessment: Concepts, modelling, applications. *Natural Hazards and Earth System Sciences*, *14*(5), 1361–1369. https://doi.org/10.5194/nhess-14-1361-2014

Uddin, K., & Matin, M. A. (2021). Potential flood hazard zonation and flood shelter suitability mapping for disaster risk mitigation in Bangladesh using geospatial technology. *Progress in Disaster Science*, *11*, 100185. https://doi.org/10.1016/j.pdisas.2021.100185

Ullah, K., & Zhang, J. (2020). GIS-based flood hazard mapping using relative frequency ratio method: A case study of Panjkora River Basin, eastern Hindu Kush, Pakistan. *PLOS ONE*, *15*(3), e0229153. https://doi.org/10.1371/journal.pone.0229153

Wei, K., Ouyang, C., Duan, H., Li, Y., Chen, M., Ma, J., An, H., & Zhou, S. (2020). Reflections on the Catastrophic 2020 Yangtze River Basin Flooding in Southern China. *The Innovation*, *1*(2), 100038. https://doi.org/10.1016/j.xinn.2020.100038

Wubalem, A., Tesfaw, G., Dawit, Z., Getahun, B., Mekuria, T., & Jothimani, M. (2021). Comparison of statistical and analytical hierarchy process methods on flood susceptibility mapping: In a case study of the Lake Tana sub-basin in northwestern Ethiopia. *Open Geosciences*, *13*(1), 1668–1688. https://doi.org/10.1515/geo-2020-0329

Yogacharya, K. S., & Gautam, D. K. (2008). *Floods in Nepal: Genesis, Magnitude, Frequency and Consequences*. https://doi.org/10.13140/RG.2.1.2376.8489